A Modified Version of L-PICOLA to Output the Gravitational Potential

Philipp Miotti*, Raphael Sgier†

Institute for Particle Physics and Astrophysics, Department of Physics,
ETH Zurich, Wolfgang-Pauli-Strasse 27, 8093 Zurich, Switzerland

February 12, 2018

Abstract

We modify the approximate N-body simulation code L-PICOLA to output the peculiar gravitational potential at the positions of the dark matter particles and on the mesh in snapshot mode. After solving the gravitational Poisson equation of the dark matter particles in a comoving frame, we find that the output potential of our pipeline is consistent with the outputted mass overdensity. The spherical harmonic power spectrum of the potential – computed from HEALPix maps of a $z = 0$ snapshot – shows an agreement within 10 % for scales $l \lesssim 30$ and $l \gtrsim 100$, and around ~ 15 % for $30 \lesssim l \lesssim 100$ between the L-PICOLA potential output and the potential from the solved Poisson equation. The average of the potential over a concentric shell from the centre of the simulation box as a function of its radius differ no more than 10 % in all shells. From the probability distribution function of the outputs we find, that the difference of the means is less than 3.3 % relatively to the RMS of their standard deviation. Our modifications can be useful to construct lensing-potential and deflection-angle maps from a fast and accurate alternative to other N-body simulations, such as GADGET-2.

Contents

*miottiph@student.ethz.ch
†rsgier@phys.ethz.ch

1 Introduction

Recent cosmological models suggest that the formation of very large structures in the universe is based on the gravitational amplification of small density perturbations. Theoretical models give analytical results on linear scales, but fail at precisely describing non-linear scales. The main tools to accurately describe the structure formation on very small scales in the non-linear regime resolved by present cosmological surveys are N-Body simulations. A simulations which meets these great demands in accuracy and performance is GADGET-2 [1]. On the other hand, a large sample of simulations is necessary to reduce the statistical noise in the covariance matrix, which is clearly limited by the computational power [5]. The new generation of approximate N-body simulations, such as L-PICOLA [2, 3, 4], provide a balance between these two needs.

The goal of this paper is to introduce modifications to L-PICOLA in order to compute and output the gravitational potential at the particle positions as well as on a 3-dimensional mesh in snapshot mode. It is a computational feature which is present in GADGET-2, but lacks in L-PICOLA yet. Knowing the gravitational potential of a simulation output is necessary to compute weak lensing maps for CMB lensing. It was found that the power spectra of approximate dark matter fields from L-PICOLA agree with that from GADGET-2 to within 5 % on all scales of interest to Baryon Acoustic Oscillation [6] and Redshift Space Distortions [7] measurements, and to within 20 % up to $k = 1.0\,h\,\mathrm{Mpc}^{-1}$ [2]. In terms of speed, so is L-PICOLA able to produce a dark matter simulation 3 orders of magnitude faster than the fully non-linear N-body simulation GADGET-2 [2].

This paper is organized as follows. In section 2 we briefly introduce the Poisson equation relating the gravitational potential with the mass overdensity and introduce dimensionless variables for our calculations. We discuss in detail the modifications to L-PICOLA we made to output the gravitational potential at the particle positions and on the mesh in section 3. Section 4 provides a description of a test simulation and tools we performed to verify the output of our modified code. We perform a statistical analysis in section 5 of the potential by computing the spherical harmonic power spectrum, the average as a function of distance from the centre of the simulation box and the probability distribution function. Lastly, the results are discussed in section 6.

2 Model equations and dimensionless variables

In this section we present the dimensionless Poisson equation of the peculiar gravitational potential ϕ of the dark matter particles (DM) for periodic boundary conditions in a comoving reference frame. This equation is solved in the Particle-Mesh (PM) algorithm of L-PICOLA [2]. For a good review and implementation of this method we refer to [8] and [9].

The dynamics of a system consisting of DM in a computational box of size L^3 is described by

$$\nabla^2\phi(\mathbf{x}) = 4\pi G\Omega_{m,0}\rho_{cr,0}\delta(\mathbf{x})a^{-1}, \quad \rho_{cr,0} = \frac{3H_0^2}{8\pi G}, \quad \delta(\mathbf{x}) \equiv \frac{\rho(\mathbf{x}) - \bar{\rho}}{\bar{\rho}}, \tag{1}$$

where $\Omega_{m,0}$ is the matter density parameter, $\rho_{cr,0}$ is the critical density and δ is the overdensity with respect to the $\Omega_{m,0}$ fraction of $\rho_{cr,0}$ at a specific time $a(t) = (1+z)^{-1}$. All cosmological parameters with a subscript $'0'$ refer to the present value ($z = 0$). In order to solve the discrete

version of Eq. (1) on a equidistant mesh, we introduce the length of a cell x_0 and the unit of time $1/H_0$ with the Hubble constant $H_0 = 100\,h\,\mathrm{km\,s^{-1}\,Mpc^{-1}}$. Now, we can cast Eq. (1) into the following dimensionless form (tildes denote dimensionless variables – code units):

$$\tilde{\nabla}^2\tilde{\phi}(\tilde{\mathbf{x}}) = \frac{3}{2}\frac{\Omega_{m,0}}{a}\left(\tilde{\rho}(\tilde{\mathbf{x}}) - 1\right), \tag{2}$$

where we used the variable transformations:

$$\mathbf{x} = x_0\tilde{\mathbf{x}}, \quad t = \tilde{t}/H_0, \tag{3}$$

$$\phi = \tilde{\phi}\left(x_0 H_0\right)^2, \quad \rho = \tilde{\rho}\frac{3H_0^2}{8\pi G}\frac{\Omega_{m,0}}{a^3}. \tag{4}$$

Now, we approximate $\tilde{\rho}$ on a discrete mesh. Let N_{mesh} and N_{sample} be the number of mesh cells and the number of particles respectively in one direction, and N the total number of particles in one cell. The density in a single cell of the box can be written as $\rho_{i,j,k} = M/x_0^3$, where $i,j,k = 1,...,N_{mesh}$ and M is the total mass inside the cell. By virtue of Eq. (4) and the particle's mass $m = \Omega_{m,0}\rho_{cr,0}\left(L/N_{sample}\right)^3$ we get $\tilde{\rho}_{i,j,k} = N\left(N_{mesh}a/N_{sample}\right)^3$. In L-PICOLA this is done by using a Cloud-in-Cell (CIC) assignment at each mesh node [2].

From this point we can solve Eq. (2) for $\tilde{\phi}$ with two methods using the discrete Fourier transform (DFT). In section 3 we will transform the equation to Fourier space from the start and then apply the discretization. The Laplace operator then converts to merely a factor $-\mathbf{k}^2$. In section 5 however, we will first write the Laplace operator in its discrete form and the and solve the equation in Fourier space.

3 Modifications of L-PICOLA

With the introduction of dimensionless equations and variables in the previous section, we are now prepared to present the modifications to L-PICOLA to output the peculiar gravitational potential at the particle positions and on the mesh for simulations in snapshot mode. First, we create a new data member for each particle and write the potential from the initial conditions in `2LPT.c` to a new variable. In file `auxPM.c` we copied the value of the potential $\tilde{\phi}$ from an intermediate step of the PM algorithm. Finally, we add this new data member to the output files in both ASCII format and unformatted binary. Like all other variables in the source file, we define new variables in `vars.c` and `vars.h`. In order to compile the modified code with the option to output the potential at the particle positions, the preprocessor directive `POTENTIAL` needs to be defined in the `Makefile`. If the potential on the mesh is requested, the directive `GONGRID` must be enabled additionally. All modifications refer to L-PICOLA v1.2, December 2015[1]. The modified version can be found at https://

The calculation of $\tilde{\phi}$ in L-PICOLA first appears in generating the initial conditions of the particles using second order Lagrangian perturbation theory (2LPT) used by the COLA method [3]. Thereby, one can choose between either Gaussian or Non-Gaussian initial conditions. No potential is computed in the Gaussian case as opposed to the Non-Gaussian case, where the value is copied to a new variable, a data member of the particle. This is done in the file `2LPT.c` of the source code.

[1] https:/cullanhowlett.github.io/l-picola.

The greatest modifications regarding the computation of $\tilde{\phi}$ were made on `auxPM.c`, where the PM algorithm is implemented. The original steps starting from the particle positions are as follows:

1. CIC interpolation to the mesh to get the mass density $\tilde{\rho}_{i,j,k}$ at each mesh point.

2. FFT of $\tilde{\rho}_{i,j,k}$ and solving Eq. (2) in Fourier-space,

$$\mathbf{k}^2\tilde{\phi}_{i,j,k}(\mathbf{k}) = \frac{3}{2}\frac{\Omega_{m,0}}{a}\tilde{\delta}_{i,j,k}(\mathbf{k}), \quad \mathbf{k} = (i,j,k)\,, \tag{5}$$

   where $\tilde{\delta}_{i,j,k}(\tilde{\mathbf{x}}) \equiv \tilde{\rho}_{i,j,k}(\tilde{\mathbf{x}}) - 1$.

3. Calculating the force at each mesh point,

$$\tilde{F}_{i,j,k}(\mathbf{k}) = \mathbf{k}\tilde{\phi}_{i,j,k}(\mathbf{k}), \tag{6}$$

   using the inverse FFT to get the force in real-space and the inverse CIC method to interpolate $\tilde{F}_{i,j,k}$ to the particle positions.

In our modification we copy the result from step 2, save it as a new variable and perform a parallel FFT using the same C libraries (FFTW[2]) as in the original code. After that, we use the inverse CIC method to interpolate the potential to the particle positions.

To output the potential at the particle positions in ASCII format we simply add a new column in the output file just after the particle positions and velocities. For data in unformatted binary format (i.e. `GADGET_STYLE` in L-PICOLA snapshot mode) the values are written as a compound block, which are associated with the particle positions through their output order. For the potential on the mesh we write a new function (under the preprocessor directive `GONGRID`) similar to that, which handles the output in snapshot mode. It writes the potential in a newly created data file (in the output folder) either in ASCII format or unformatted binary. The function is called at every output redshift.

In the next section we will show a snapshot simulation with the above mentioned modifications, i.e the gravitational potential at the particle positions. The results are also representative for a test simulation of the potential on the mesh, as they merely differ in the CIC interpolation used.

4 Test simulation

After we presented our modifications to L-PICOLA in the previous section, we now show the results of a simulation outputting the potential at the particle positions at redshift $z = 0$. We therefore run a simulation (with the COLA method enabled) from $z = 9$ to $z = 0$. The box has a edge length of $L = 100\,h^{-1}\,\mathrm{Mpc}$ with $N_{sample} = 128$ particles and a mesh size $N_{mesh} = 128$ in one dimension. Further we set the matter density parameter $\Omega_{m,0} = 0.276$, the Hubble parameter $h = 0.7$, the power spectrum normalization $\sigma_8 = 0.83$ and primordial index $n_s = 0.96$. Then, we plot the potential with the HEALPix[3] hierarchical tessellation of the unit sphere [10].

[2] http://www.fftw.org/

[3] http://healpix.sourceforge.net

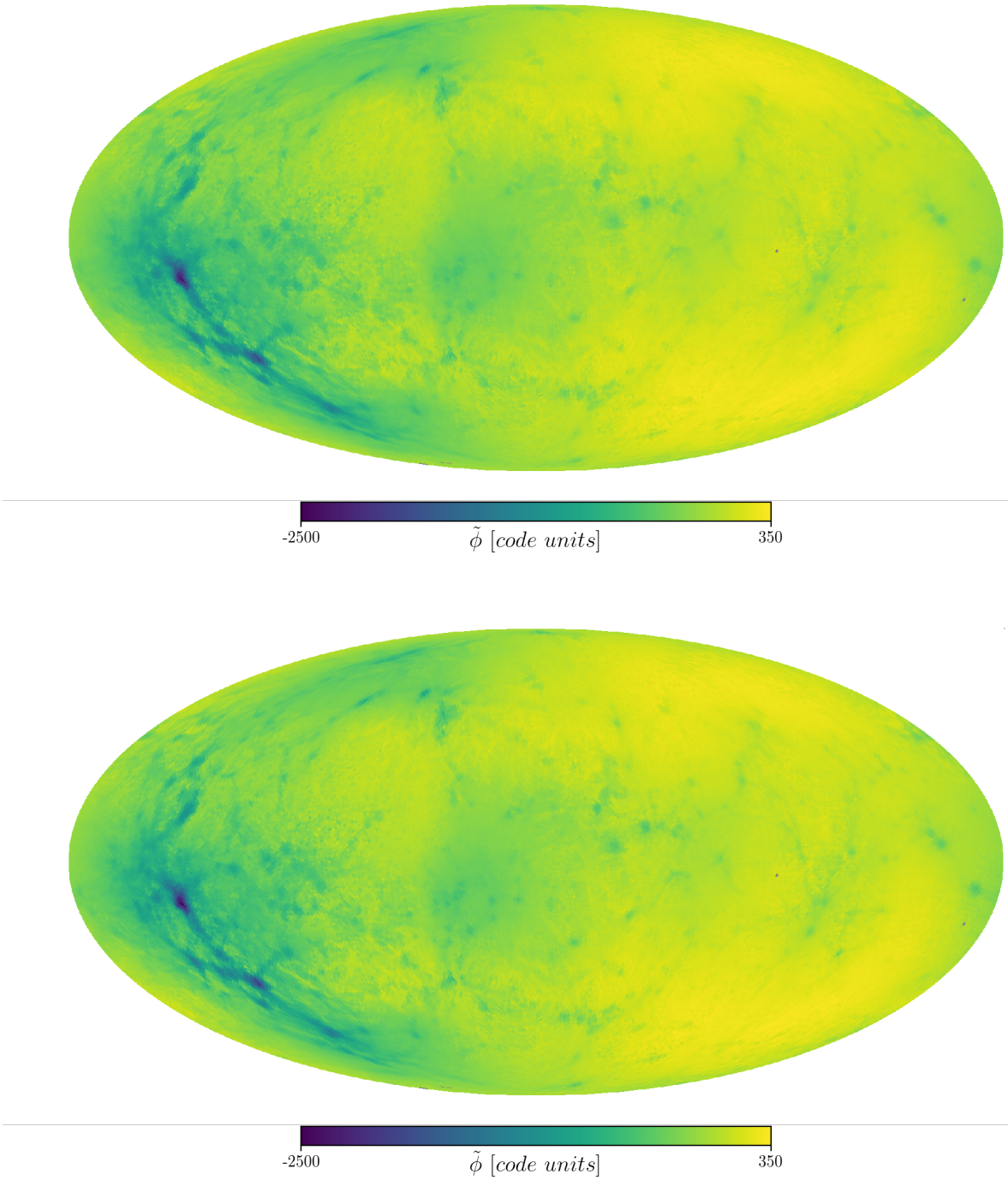

Figure 1: All-sky maps of the gravitational potential from data of L-PICOLA. *Top image:* Potential in code units obtained from the code output directly. *Bottom image:* Potential in code units obtained from the particle positions after solving Eq. (7).

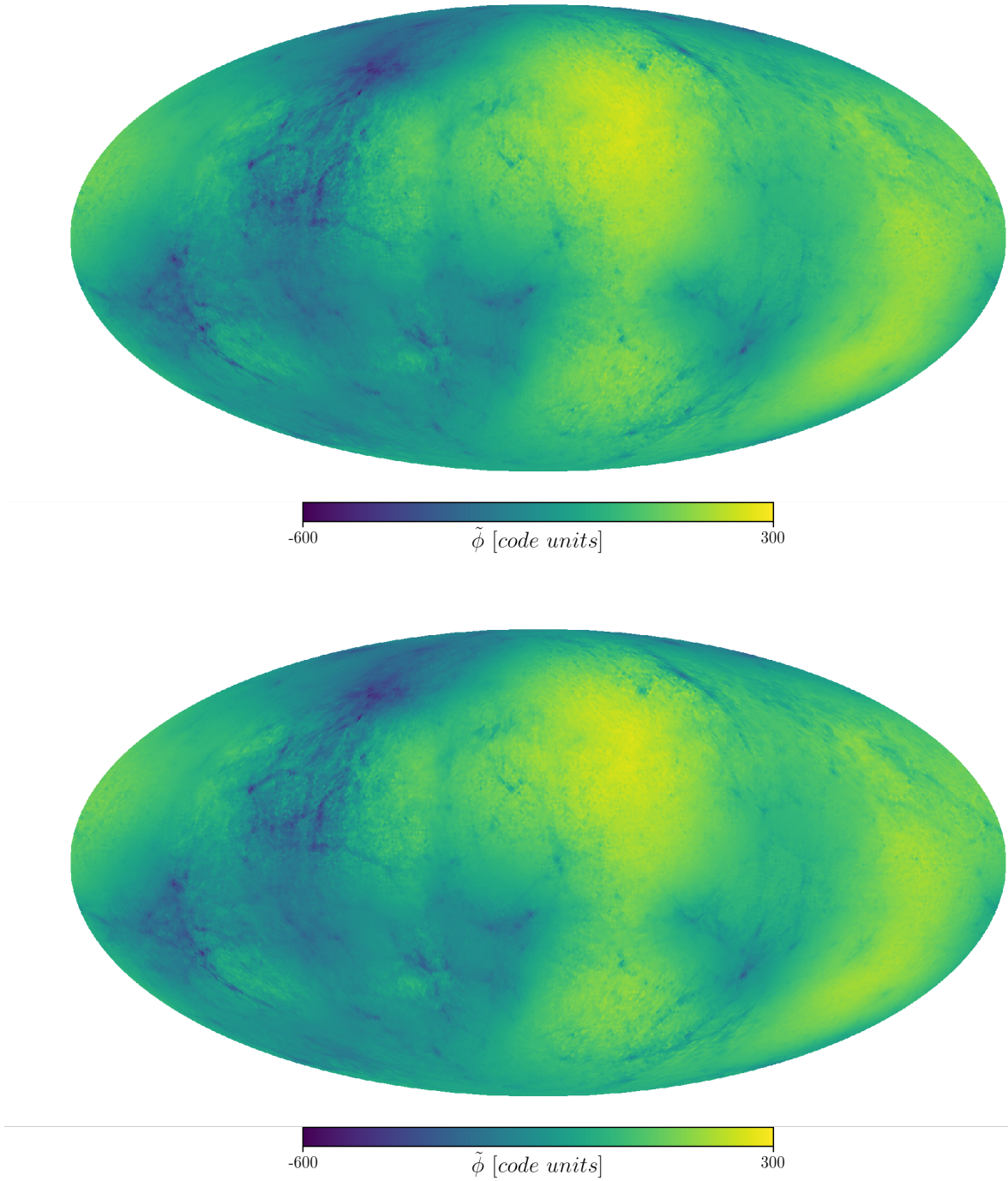

Figure 2: All-sky maps of the gravitational potential from data of GADGET-2. *Top image:* Potential in code units obtained from the code output directly. *Bottom image:* Potential in code units obtained from the particle positions after solving Eq. (7).

In the top image of Fig. 1 we show the gravitational potential in code units $\tilde{\phi}$ (see section 2 for details) of the L-PICOLA simulation up to an arbitrary constant. The map was first generated with a HEALPix pixelization parameter $N_{side} = 2^9$, which corresponds to 3145728 pixels. This is enough to plot all $N^3_{sample} = 2097152$ data points. Then we use a HEALPy function `pixelfunc.ud_grade` to degrade the resolution to $N_{side} = 2^6$, corresponding to 49152 pixels with a resolution of ~ 54.98 arcmin. The blue color in the image represent regions of potential wells, i.e. regions of high mass density.

The bottom image of Fig. 1 shows the same simulation box. However, here we use the particle positions as input data for the pipeline to generate this plot. Besides the mapping procedure described in the last paragraph, this pipeline consist of the following steps:

1. We use the CIC method to interpolate the particle positions to the mesh, thus getting the mass density $\tilde{\rho}_{i,j,k}$ $(i, j, k = 1, ..., N_{mesh})$.

2. We solve Eq. (2) in Fourier-space with a discretized Laplace operator, $\tilde{\nabla}^2\tilde{\phi}(\tilde{\mathbf{x}}) \simeq \tilde{\phi}_{i+1,j,k} + \tilde{\phi}_{i-1,j,k} + \tilde{\phi}_{i,j+1,k} + \tilde{\phi}_{i,j-1,k} + \tilde{\phi}_{i,j,k+1} + \tilde{\phi}_{i,j,k-1} - 6\tilde{\phi}_{i,j,k}$, yielding for the transformed potential,

$$\tilde{\phi}_{i,j,k}(\mathbf{k}) = \frac{3}{2}\frac{\Omega_{m,0}}{a}\frac{\tilde{\delta}_{i,j,k}(\mathbf{k})}{\omega^i + \omega^{-i} + \omega^j + \omega^{-j} + \omega^k + \omega^{-k} - 6}, \quad \omega \equiv e^{2\pi i/N_{mesh}}. \tag{7}$$

3. We transform $\tilde{\phi}_{i,j,k}(\mathbf{k})$ back to real-space and use the inverse CIC interpolation to get the potential at the particle positions.

The above pipeline was implemented in Python using the FFT libraries from NumPy. The transformations were performed with 128 equidistant sample points in each dimension and the full complex Fourier transform, which is appropriate for problems satisfying periodic boundary conditions. With this approach we want to prove that the potential computed with the modified L-PICOLA is consistent with the particle distribution. No difference can be found just by looking at the two maps. We will provide a more detailed analysis in the next section.

To check that we have not made an error in our calculations, we run the same simulation box using the same parameters and cosmological model with GADGET-2. Although the seed for the particle positions was the same as in L-PICOLA, major differences in the algorithmic calculation of the particle interactions – splitting the potential into a long-range and short-range part – have not allowed us to compare them [1]. The results are shown in Fig. 2 using the same procedure as for L-PICOLA.

5 Analysis and verification

To compare the results presented in Fig. (1) and (2), we calculate the spherical harmonic power spectrum using the HEALPy function `sphtfunc.anafast`. The spectrum is taken from 49152 pixels corresponding to a resolution of ~ 54.98 arcmin. The results are plotted in Fig. (3). Except for the monopole, we see a less than 10 % discrepancy – relative to *simulation* output – over all scales between the GADGET-2 outputs. The reason for the anomaly in the monopole could be the overall error ~ 0.44 in $\tilde{\phi}$ made by our Poisson solver described in the previous section. The error is estimated from solving the Poisson equation,

$$\nabla^2 f(x, y, z) = 2\left(2x^2 + 2y^2 + 2z^2 - 3\right) f(x, y, z), \quad f(x, y, z) \equiv e^{-\left(x^2+y^2+z^2\right)}, \tag{8}$$

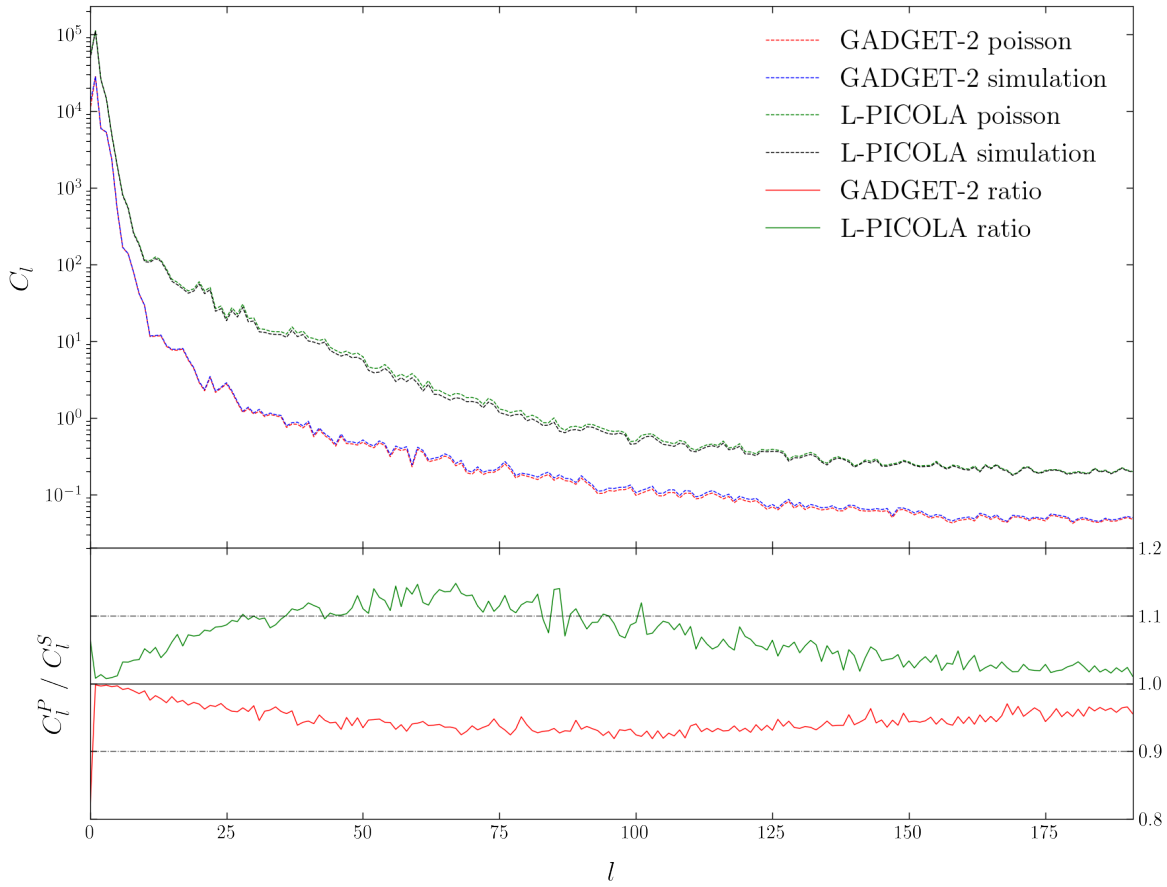

Figure 3: Spherical harmonic power spectrum of the gravitational potential from the HEALPix maps in Fig. 1 and 2 with an angular resolution of ~ 54.98 arcmin. In the upper panel we compare the spectrum of $\tilde{\phi}$ from the simulation output (*simulation*) to the result of Eq. (7) (*poisson*) for both L-PICOLA and GADGET-2. In the lower panel we take the ratio of *simulation* and *poisson*.

on an equidistant mesh with 128 samples in each dimension. For L-PICOLA we get similar results. However, due to higher gradients of the potential compared to GADGET-2, the spectra differ more than 10 % – relative to *simulation* output – on scales $30 \lesssim l \lesssim 100$ and there is also an excess in the monopole.

The spectrum gives only a 2-dimensional analysis of the potential on the unit sphere. To investigate $\tilde{\phi}$ also in r-dimension, we divide the simulation box into 100 concentric shells around its centre, such that the outmost shell completely covers the box. We then take the average of $\tilde{\phi}$ in each shell and plot it as a function of the radius of the shell's mid-layer. These averages $\langle\tilde{\phi}\rangle_{shell}$ from the simulation output (*simulation*) and the calculated potential by the Poisson solver (*poisson*) – as well as their ratio – are shown in Fig. 4 for both L-PICOLA and GADGET-2. In the lower panel we see that the results from GADGET-2 agree within 5 % – relative to *simulation* output – for all radii. The averages $\langle\tilde{\phi}\rangle_{shell}$ from L-PICOLA vary within 10 % – relative to *simulation* output – for all radii. By comparing this plot with the

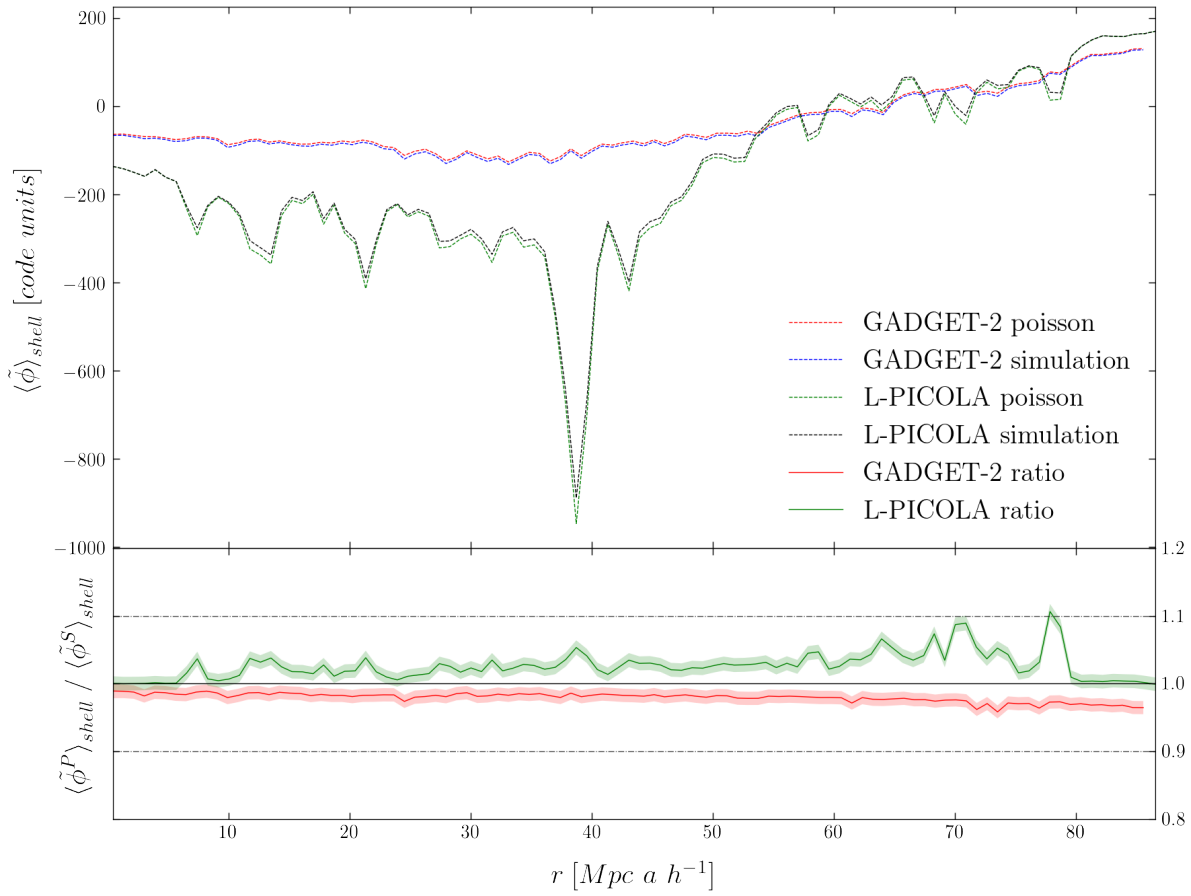

Figure 4: Gravitational potential averaged over concentric shells with the centre of the simulation box as the origin and a shell thickness $\sim 0.87\,\mathrm{Mpc\,a\,h^{-1}}$. In the upper panel we compare $\langle\tilde{\phi}\rangle_{shell}$ from the simulation output (*simulation*) to the result of Eq. (7) (*poisson*) for both L-PICOLA and GADGET-2. In the lower panel we take the ratio of *simulation* and *poisson*. The red and green area represent the largest error in solving Eq. (7) for GADGET-2 and L-PICOLA respectively.

one in Fig. 3, we notice that the potential wells from the Poisson solver are more distinctive than the wells from the simulation in case of L-PICOLA. The opposite is true for the results of GADGET-2. One explanation for this tendency could by that the solver performs better on smooth scalar fields, as in the case of GADGET-2. To investigate this hypothesis we suggest trying to use more sample points for the FFT.

Furthermore, we compare the probability distribution function (PDF) of the potential from the simulation output (*simulation*) to the one from the Poisson solver (*poisson*) for both codes. The results are shown in Fig. 5. The PDF's are plotted against 200 bins with size 19.25. We find that the $\tilde{\phi}$-values of the two outputs share a similar distribution for either simulation code. In Tab. 1 the sample means and standard deviations of $\tilde{\phi}$ of the two outputs and simulation codes are presented. In the lower panel of Fig. 5 we compare the PDF's. The weighted average of their relative difference – relative to PDF($\tilde{\phi}^S$) – is less than 2.5 % and less than 5 %, while

the difference of the means relatively to the RMS of their standard deviation is less than 2.9 % and less than 3.3 % for GADGET-2 and L-PICOLA respectively.

f	$\tilde{\phi}^{poisson}_{GADGET-2}$	$\tilde{\phi}^{simulation}_{GADGET-2}$	$\tilde{\phi}^{poisson}_{L-PICOLA}$	$\tilde{\phi}^{simulation}_{L-PICOLA}$
$\langle f \rangle$	-58.31	-63.30	-216.09	-203.91
σ_f	151.15	153.87	434.73	415.28

Table 1: Sample mean $\langle f \rangle$ and standard deviation σ_f of the gravitational potential for the various outputs and simulation codes.

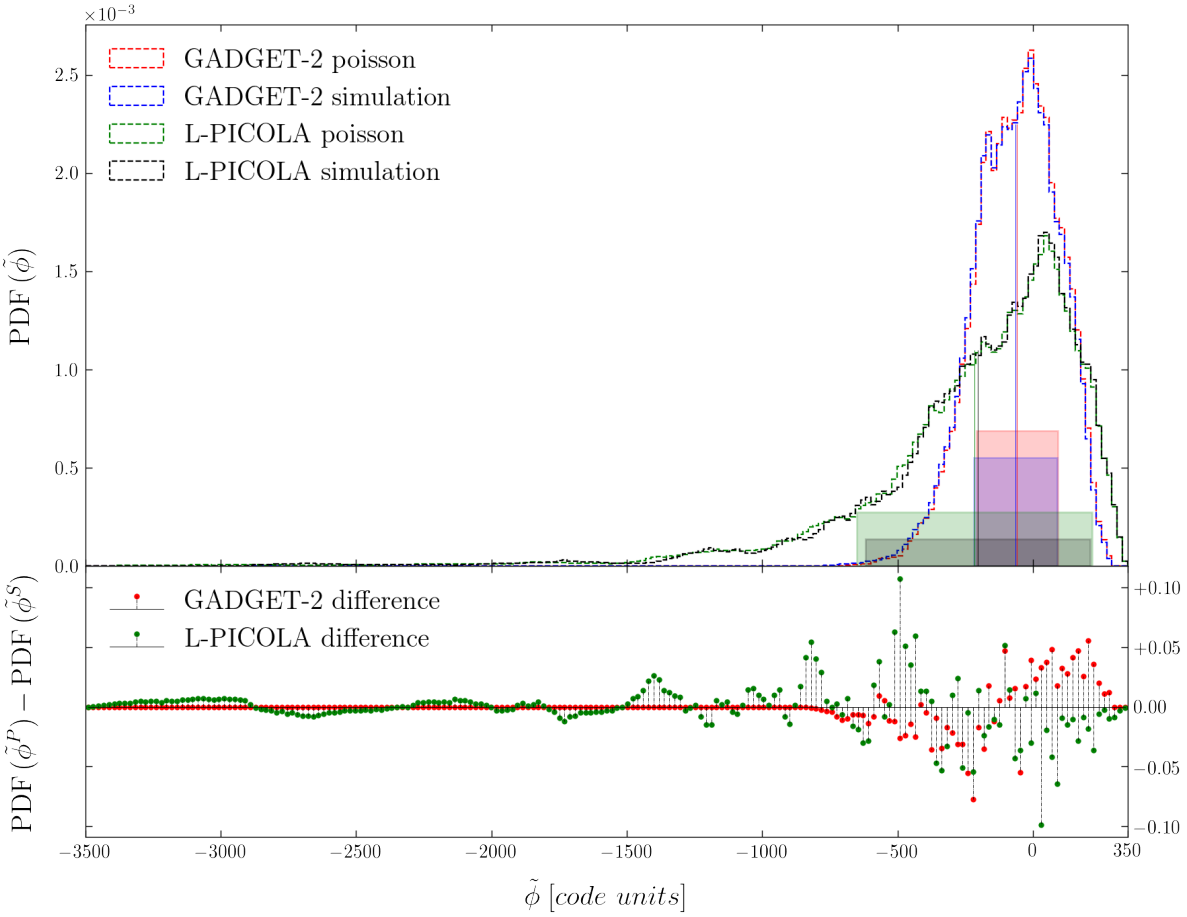

Figure 5: PDF of the gravitational potential. In the upper panel we compare the PDF $(\tilde{\phi})$ from the simulation output (*simulation*) to the result of Eq. (7) (*poisson*) for both L-PICOLA and GADGET-2. The solid vertical lines pinpoint the sample means of the potentials $\langle\tilde{\phi}\rangle$ and the half base-length of the colored rectangles the unbiased standard deviation $\sigma_{\tilde{\phi}}$ for the various outputs. In the lower panel the difference of the PDF's of the results is shown. The bin size is 19.25. The y-axis of both plots is scaled to 10^{-3}.

6 Conclusion

In this paper we introduced a modification of L-PICOLA to output the peculiar gravitational potential at the particle positions and on an equidistant mesh. This could be useful for future constructions of all-sky lensing-potential and deflection-angle maps. Also, to help N-body simulations to directly simulate the CMB distortions caused by weak lensing much faster and thus provide enough simulation samples to increase the statistical significance of cosmological CMB surveys. We run this modified version on $\left(100\,h^{-1}\,\mathrm{Mpc\,a}\right)^3$ volume of space with 2097152 dark matter particles. The same simulation was also done using GADGET-2. We then looked at a single snapshot output at $z = 0$ to investigate the gravitational potential at the particle positions. This result then also induces the correctness of the potential on the mesh, as they merely differ by a Cloud-in-Cell interpolation method. To prove that our modifications are correct, we solved the Poisson equation of the potential using the mass overdensity field from the particle positions of the simulation output. The GADGET-2 simulation was used to show that we did not make any systematical error in the Poisson solver implemented in Python. With the analysis of the spherical harmonic power spectrum from the HEALPix maps of the potential we found an agreement $C_{l,poisson}^{L-PICOLA}/C_{l,simulation}^{L-PICOLA} < 10\,\%$ on scales $l \lesssim 30$ and $l \gtrsim 100$. The discrepancy around $\sim 15\,\%$ for $30 \lesssim l \lesssim 100$ is due to the small sampling of the FFT in the Poisson solver and the bump of the monopole $l = 0$ are caused by an error of ~ 0.44 in the potential made by the solver as well. Furthermore, to complement the analysis in all 3 dimensions, we computed the average of the potential over a concentric shell from the centre of the simulation box as a function of its radius. The potential varied within 10 % relative to the simulation output in all shells. Lastly, we took the 1-point distribution (PDF) of the potential. The difference of the means relatively to the RMS of their standard deviation is less than 2.9 % and less than 3.3 % for GADGET-2 and L-PICOLA respectively. The distributions show that the weighted average of the relative difference between the PDF – relative to PDF($\tilde{\phi}^S$) – of the simulation output and the PDF of the calculated potential from the Poisson solver is less than 2.5 % and less than 5 % for GADGET-2 and L-PICOLA respectively. Thus we conclude that our modified version of L-PICOLA is able to produce a gravitational potential field, as well as to sample the potential at the position of the particles. A further improvement of L-PICOLA would be to transfer our pipeline to generate a simulation with the potential in lightcone mode.

Acknowledgments

We would like to thank Uwe Schmitt for his help with the computing implementation. This research made use of MUSIC[4] [11], IPython, Jupyter notebook, NumPy, SciPy, Matplotlib, Healpy, Pynbody.

[4]To generate initial conditions for GADGET-2.

References

[1] Springel V., *The Cosmological Simulation Code GADGET-2, MNRAS* **364** (2005) 1105-1134.

[2] Howlett C., Manera M. & Percival W.J., *L-PICOLA: A Parallel Code for Fast Dark Matter Simulation*, arXiv:1506.03737.

[3] Tassev S., Zaldarriaga M. & Eisenstein D., *Solving Large Scale Structure in Ten Easy Steps with COLA, JCAP* **06** (2013) 036.

[4] Scoccimarro R., Hui L., Manera M. & Chan K.C., *Large-scale Bias and Efficient Generation of Initial Conditions for Nonlocal Primordial non-Gaussianity, Phys. Rev. D* **85** (2012) 083002, arXiv:1108.5512.

[5] Sgier R.J., Réfrégier A., Amara A. & Nicola A., *Fast Generation of Covariance Matrices for Weak Lensing*, arXiv:1801.05745v1

[6] Seo H.-J., Eisenstein D.J., *Probing Dark Energy with Baryonic Acoustic Oscillations from Future Large Galaxy Redshift Surveys ,ApJ* **598** (2003) 720

[7] Kaiser N., *Clustering in real space and in redshift space, MNRAS* **227** (1987) 1

[8] Hockney R.W. & Eastwood J.W., *Computer Simulation using Particles*, (1988)

[9] Klypin A.A. & Holtzmann S.F., *Particle-Mesh Code for Cosmological Simulations*, arXiv:astro-ph/9712217.

[10] Gorski K.M., *HEALPix: A Framework for High-Resolution Discretization and Fast Analysis of Data Distributed on the Sphere, Astrophys. J.* **622** (2005) 759.

[11] O. Hahn and T. Abel, *Multi-scale initial conditions for cosmological simulations, MNRAS* **415** (2011) 2101-2121